NEUTRAL STRANGE PARTICLE PRODUCTION IN π^-d INTERACTIONS AT 21 GeV/c

By P. Stopa

Institute of Nuclear Physics, High Energy Physics Laboratory, Cracow*

(*Received August 25, 1986*)

The production of K^0_S, Λ^0, and $\bar{\Lambda}^0$ in π^-d interactions at 21 GeV/c is investigated. Cross sections for single neutral strange particles and their pairs are determined both inclusively and as functions of the charged multiplicity. Inclusive, single particle distributions show the same general features as in $\pi^\pm$p interactions (in hydrogen). The effects of double scattering are estimated. The neutral strange particle production in π^-n collisions has been extracted from deuterium data and compared with isospin symmetric π^+p reaction (in hydrogen) at similar energies. The polarization of Λ^0 has been found negligible except for Λ^0 produced in the backward hemisphere at large p_t. The Feynman x distributions of neutral strange particles both in beam and target fragmentation regions are compared with the quark counting rules predictions.

PACS numbers: 13.85.Ni

1. *Introduction*

There are many papers published on inclusive neutral strange particle production in nonstrange hadron collisions with hydrogen target in a large energy range: π^-p 2–360 GeV/c [1–17], π^+p 4–147 GeV/c [11, 18–23], pp 5–405 GeV/c [24–35] and $\bar{\text{p}}$p 1–100 GeV/c [36–40] from bubble chamber experiments, and for highest energy available in pp at CERN ISR [41] and $\bar{\text{p}}$p at CERN collider [42]. However much less experimental data on strange particle production exist for deuterium target. The only data published are: one paper on π^-d interactions at 205 GeV/c [43], one on π^+d at 24 GeV/c [44] and very few on pd [45–46].

The experiments with deuterium are interesting mainly for two reasons:

(*i*) deuteron, the simplest nucleus which consists of loosely bound proton and neutron, is the best tool for the investigation of nuclear double scattering effects,

* Address: Instytut Fizyki Jądrowej, Zakład V, Kawiory 26a, 30-055 Kraków, Poland.

(*ii*) collisions with deuteron are practically the only source of data on meson-neutron interactions.

The inclusive sample of neutral strange particles produced on deuterium results from three different processes (we assume that coherent production can be neglected):

(*i*) single collision with proton; neutron called "spectator" does not take part in the reactions and has Fermi momentum in the final state,

(*ii*) single interaction with neutron, proton remaining as "spectator",

(*iii*) double scattering, i.e. consecutive collisions with both nucleons.

The analysis is therefore more complicated than in the case of hydrogen target and the eventual difference could come mainly from nuclear effects since one expects similar strange particle production in π^-n interactions as in the isospin symmetric π^+p reaction.

2. *Experimental procedure*

The analysis has been performed using a part of the film (68000 pictures) taken by the Cambridge–Cracow–Warsaw Collaboration at CERN. The deuterium-filled 2m bubble chamber has been exposed to an unseparated π^- beam of 21 GeV/c momentum. The experimental set-up and general data analysis has been presented in a previous publication [47]. The film was scanned in three views for all primary interactions inside the fiducial volume of $133 \times 99 \times 43$ cm^3 and associated neutral particle decays V^0 and electron pairs from photon conversion. Slow proton tracks ($p < 1.5$ GeV/c) identified by ionization and tracks from the V^0 decay and γ conversion associated with the primary vertex were measured for all events and then processed by the geometric reconstruction (THRESH [48]) and kinematics (GRIND [49]) programs. All the V^0 decays were fitted with the K^0_S, Λ^0, $\bar{\Lambda}^0$ and electron pair hypotheses. Only "3c fits" with probability greater than 1% were accepted. In order to reduce the number of ambiguous fits the selection criteria based on ionization of decay products and kinematic correlations (Armenteros-Podolansky plot [50]) have been applied. The finally accepted sample of V^0 fits contained 421 K^0_S/Λ^0 ambiguous events (11% of all accepted K^0_S fits, 20% of all Λ^0) and 152 $K^0_S/\bar{\Lambda}^0$ (5% of all K^0_S, 60% of $\bar{\Lambda}^0$ fits). Those ambiguous events were included with hypothesis weights resulting from the relative densities of K^0_S, Λ^0 and $\bar{\Lambda}^0$, K^0_S in their common regions on Armenteros-Podolansky plot: $W(\Lambda^0) = 0.85$, $W(K^0_S) = 0.15$ for K^0_S/Λ^0 and $W(\bar{\Lambda}^0) = 0.25$, $W(K^0_S) = 0.75$ for $K^0_S/\bar{\Lambda}^0$ ambiguity. No V^0/γ ambiguity was left.

In order to estimate the total number of produced neutral strange particles the selected sample of V^0 decays was corrected to allow for:

1) losses due to decays too close to the primary vertex (a cut-off length of 0.5 cm was applied) or out of the fiducial volume; the average decay weights for K^0_S, Λ^0, and $\bar{\Lambda}^0$ were: 1.12 ± 0.02, 1.12 ± 0.2, 1.17 ± 0.05, respectively;

2) losses due to neutral decays of strange particles;

3) losses due to decays missed in the scan (the efficiences for finding V^0 were 96 ± 3.8% in double and 81 ± 3.2% in single scan);

4) unmeasurable events, losses in the data processing; here the so-called "passing--rate" was 83%.

3. *Cross sections and multiplicities*

Table I lists the numbers of K_S^0, Λ^0 and $\overline{\Lambda}^0$ used in the analysis and the obtained inclusive neutral strange particle cross-sections for each number of charged particles in a final state. They have been determined using topological cross-sections $\sigma_n(\pi^- d \to n$ charged particles + anything) published previously [47]. It was assumed that the microbarn equivalent of the event $R_\mu(n)$ found in this way was the function of charged multiplicity only, thus the inclusive cross-section for production of V^0 with n charged particles was

$$\sigma^V_{inc}(n) = R_\mu(n) \cdot N_V(n),$$

where $N_V(n)$ is the total number of events with V^0 and charged multiplicity n (corrected for all possible losses as indicated in previous Chapter). The inclusive cross-sections for production of pairs of neutral strange particles obtained similarly are shown in Table II. Fig. 1 displays the topological cross-sections (normalized to the inelastic cross-section) as a function of negative particle multiplicity n_-. The dependence on n_- looks very similar for K_S^0, Λ^0, $\overline{\Lambda}^0$ and overall π^-d topological cross-sections. The curves in Fig. 1 show the topological cross-sections for π^-p interactions at 18.5 GeV/c [11] (for comparison). It is seen that the distributions for π^-d are broader: there is a bigger strange particle yield in π^-d than in π^-p at higher multiplicities. Since it was shown [47] that the rate of double scattering in deuterium increases at high multiplicities, this excess of strange particle production in high multiplicity π^-d collisions may at least partly come from double scattering.

The average values $\langle n_{ch} \rangle$ and dispersions D of multiplicity distribution of charged

TABLE I

Semi-inclusive production cross-section for K_S^0, Λ^0, and $\overline{\Lambda}^0$

	K_S^0		Λ^0		$\overline{\Lambda}^0$	
Charged multiplicity	Number of decays	$\sigma_{incl}[\mu b]$	Number of decays	$\sigma_{incl}[\mu n]$	Number of decays	$\sigma_{incl}[\mu b]$
0	34	85.6±16.5	30	96.8±19.6	5	9.6±4.7
1	110	181.5±20.5	52	92.7±14.2	19	26.9±8.8
2	606	762.1±49.7	356	493.0±36.3	43	43.6±7.7
3	414	363.7±26.1	229	236.2±20.0	31	22.3±4.6
4	1019	997.0±58.6	556	573.0±37.8	85	54.0±7.0
5	390	319.2±23.3	198	187.1±16.6	19	9.0±2.4
6	690	586.6±37.3	416	426.6±30.2	30	17.0±3.6
7	128	106.2±11.2	75	74.0±9.6	8	5.2±2.0
8	233	200.8±16.9	135	140.3±14.3	9	3.5±1.5
9	22	20.6±4.6	19	19.7±4.8		
10	46	40.8±6.5	32	34.7±6.5	3	0.7±0.4
11	3	1.8±1.3	3	3.4±1.8		
12	6	5.0±2.2	4	3.5±1.5		
total	3781	3671±195	2105	2381±131	252	192±18

TABLE II

Semi-inclusive cross-sections for neutral strange particle pairs production

Charged multiplicity	$K_S^0K_S^0$		$K_S^0\Lambda^0$		$K_S^0\bar{\Lambda}^0$		$\Lambda^0\bar{\Lambda}^0$	
	Number of pairs	$\sigma_{incl}[\mu b]$	Number of pairs	$\sigma_{incl}[\mu b]$	Number of pairs	$\sigma_{incl}[\mu b]$	Number of pairs	$\sigma_{incl}[\mu b]$
0	2	7.0±4.8	4	21.6±10.9	2	1.1±0.8	2	7.6±5.3
1	15	32.3±8.7	12	39.1±11.5	1	0.7±0.7	2	4.6±3.3
2	55	96.9±12.0	65	150.3±20.3	9	15.1±5.3	10	15.5±5.1
3	38	47.6±8.3	35	57.2±10.8	3	2.5±1.4	4	4.8±2.5
4	81	104.5±12.9	91	154.2±18.2	13	9.3±2.7	9	11.1±4.0
5	28	33.6±6.7	18	23.2±5.7				
6	39	42.4±7.3	45	71.7±11.4	2	0.6±0.4	2	2.0±1.5
7	6	6.3±2.8	9	12.6±4.3				
8	6	6.1±2.8	17	30.8±7.7	1	0.4±0.4	1	0.4±0.4
10	2	1.9±1.5	4	7.5±3.9				
total	272	378±31	301	570±45	31	29.7±5.9	30	46.0±9.3

particles produced in reactions with seen K_S^0, Λ^0 and $\bar{\Lambda}^0$ decays are listed in Table III together with those from the 16 GeV/c π^-p experiment [10]. The average charged multiplicities are equal for Λ^0 and K_S^0 samples, smaller for $\bar{\Lambda}^0$, all being smaller than the overall π^-d average charged multiplicity. This suggests the important role of phase space constraints at this rather low energy. Both D and $\langle n_{ch}\rangle_V$ are greater in π^-d than in π^-p reactions for all types of the V^0 events, however the ratio $D/\langle n_{ch}\rangle$ remains constant and equal to about

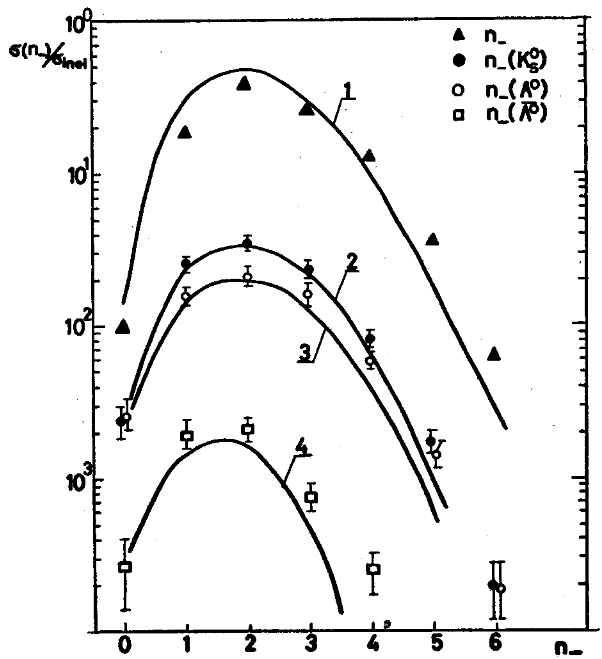

Fig. 1. Topological cross-sections $\sigma_{n_-}(\pi^-d)$ for production of n_- negative particles divided by the inelastic cross-section $\sigma_{in}(\pi^-d)$ for: all events (triangles), events with K_S^0 (full circles), events with Λ^0 (circles), events with $\bar{\Lambda}^0$ (squares). The curves 1, 2, 3, 4 are the respective cross-sections for π^-p 18.5 GeV/c [11] divided by $\sigma_{in}(\pi^-p)$

TABLE III

Average multiplicity and dispersion of charged particles: total and associated with V^0 produced in π^-p and π^-d interactions

	$\langle n_{ch}\rangle$		D	
	π^-d at 21 GeV/c	π^-p at 16 GeV/c	π^-d at 21 GeV/c	π^-p at 16 GeV/c
total	4.45±0.04	4.20±0.06	2.16±0.05	1.88±0.08
K_S^0	4.07±0.04	3.60±0.16	2.11±0.03	1.91±0.13
Λ^0	4.12±0.05	3.58±0.18	2.20±0.05	1.94±0.15
$\bar{\Lambda}^0$	3.25±0.12	2.76±0.21	1.80±0.13	1.48±0.22

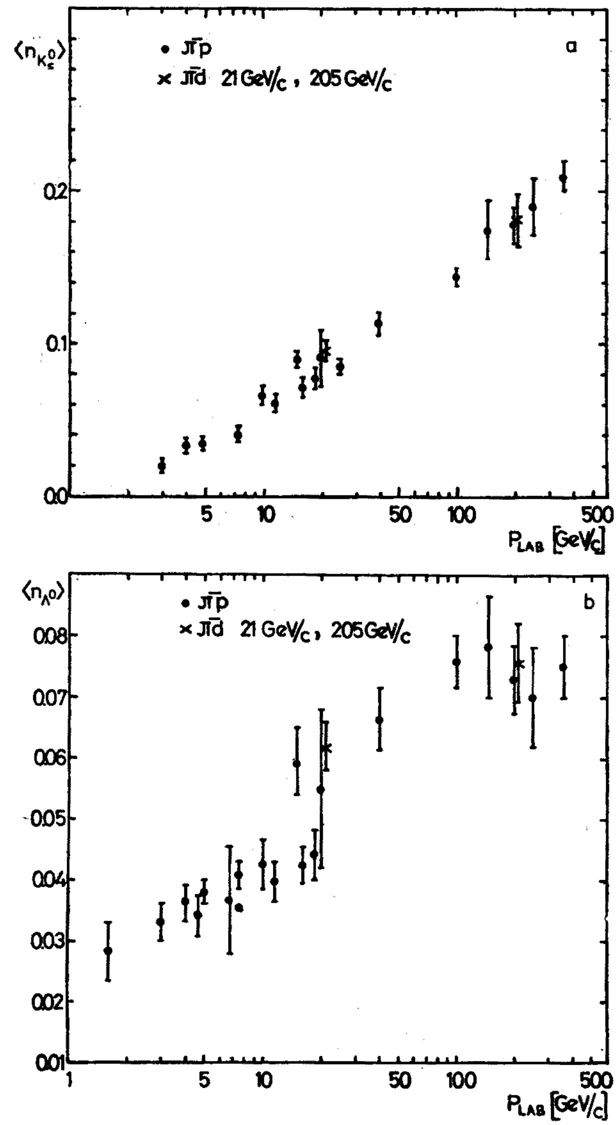

Fig. 2a, b. Average multiplicities of neutral strange particles produced in π^-p and π^-d interactions vs π^- beam momentum p_{LAB}, for: a) K_S^0, b) Λ^0

0.5 which is consistent with the general observation made for hadron–hadron collisions by Wróblewski [51]. The average production rates of neutral strange particles Λ^0, K_S^0 and $\bar{\Lambda}^0$ per inelastic π^-d collision as a function of negative particle multiplicity n_- are presented in Table IV. All these average multiplicities of V^0 show a decrease with increasing n_- already observed in π^-p interactions at similar energies. The average multiplicities of K_S^0, Λ^0; and $\bar{\Lambda}^0$ produced in π^-d reactions are compared (Figs 2a, b, c) with π^-p data [1–17] from the whole energy range available: 2–360 GeV. The points for deuterium are consistent with the interpolation of the π^-p data.

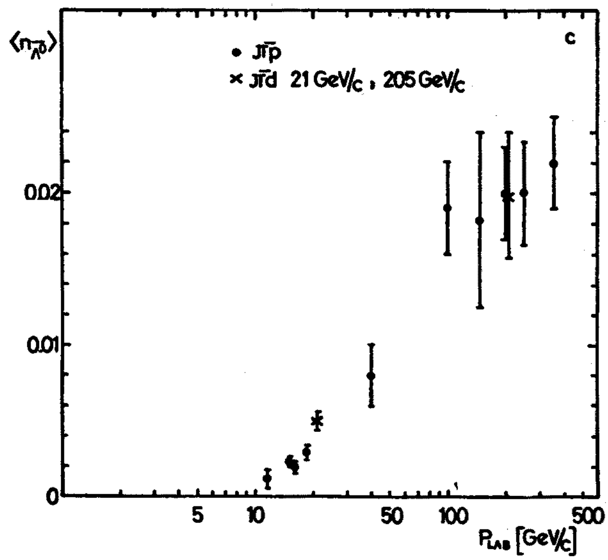

Fig. 2c. Average multiplicities of neutral strange particles produced in π^-p and π^-d interactions vs π^- beam momentum p_{LAB}, for $\bar{\Lambda}^0$

TABLE IV

Average neutral strange particle multiplicities as a function of negative particle multiplicity n_-

n_-	Number of events	$\langle K^0_S \rangle$	Number of events	$\langle \Lambda^0 \rangle$	Number of events	$\langle \bar{\Lambda}^0 \rangle$
0	34	0.239 ± 0.048	30	0.263 ± 0.057	5	0.0267 ± 0.0130
1	716	0.135 ± 0.021	408	0.084 ± 0.013	62	0.0100 ± 0.0020
2	1513	0.096 ± 0.006	785	0.057 ± 0.004	116	0.0054 ± 0.0006
3	1080	0.088 ± 0.005	614	0.059 ± 0.005	49	0.0025 ± 0.0005
4	361	0.064 ± 0.005	210	0.045 ± 0.005	17	0.0018 ± 0.0006
5	68	0.046 ± 0.006	51	0.040 ± 0.006	3	0.0006 ± 0.0004
6	9	0.029 ± 0.011	7	0.028 ± 0.010		
all	3781	0.096 ± 0.006	2105	0.061 ± 0.004	262	0.0048 ± 0.0005

The ratio of average multiplicities of K^0_S and π^0 in π^-d 21 GeV is also similar as in π^-p interactions at comparable energies [52] amounting to

$$\frac{\langle K^0_S \rangle}{\langle \pi^0 \rangle} = 0.045 \pm 0.005.$$

4. *Differential distributions*

All inclusive distributions presented in this paper are in the π^--nucleon centre of mass system (assuming the nucleon in the deuteron target at rest). In reality the nucleons bound in deuteron have some Fermi momentum which can be well parametrized by the well-

-known Hulthén distribution [53]. It was found however by Monte Carlo calculation that the influence of the Fermi motion of the target-nucleon on the rapidity, Feynman x and transverse momentum distributions is negligible.

The invariant rapidity distribution for Λ^0, K_S^0, and $\bar{\Lambda}^0$

$$F(y_{cm}) = \frac{1}{\pi} \int \frac{d^3\sigma}{dy_{cm} dp_t^2} \, dp_t^2$$

is shown in Fig. 3a, b. The curves drawn denote the respective distributions for neutral strange particles produced in π^-p interactions at 18.5 GeV [11] multiplied by the ratio of the inelastic cross-sections $\sigma_{in}(\pi^-d)/\sigma_{in}(\pi^-p)$. The shapes of all distributions for π^-d are very similar to those for π^-p. It is seen that the neutral kaons are produced mainly forward in CMS in the π^- beam fragmentation region with a big contribution of central production. Similar features has $\bar{\Lambda}^0$ production which however is more central. In contrast to that, the Λ^0 particles are mostly produced backwards (in the CMS), and the target fragmentation seems to be the dominant Λ^0 production mechanism.

A more quantitative description of those production features can be given in terms of the asymmetry parameter

$$A = \frac{F-B}{F+B},$$

where F (B) denotes the fraction of the inclusive cross-section in the forward (backward) hemisphere in CMS. The values of A given in Table V are small, positive for K_S^0 and $\bar{\Lambda}^0$, bigger, negative for Λ^0 in all reactions compared: $\pi^\pm p$, $\pi^\pm d$ and νp [54]. The absolute

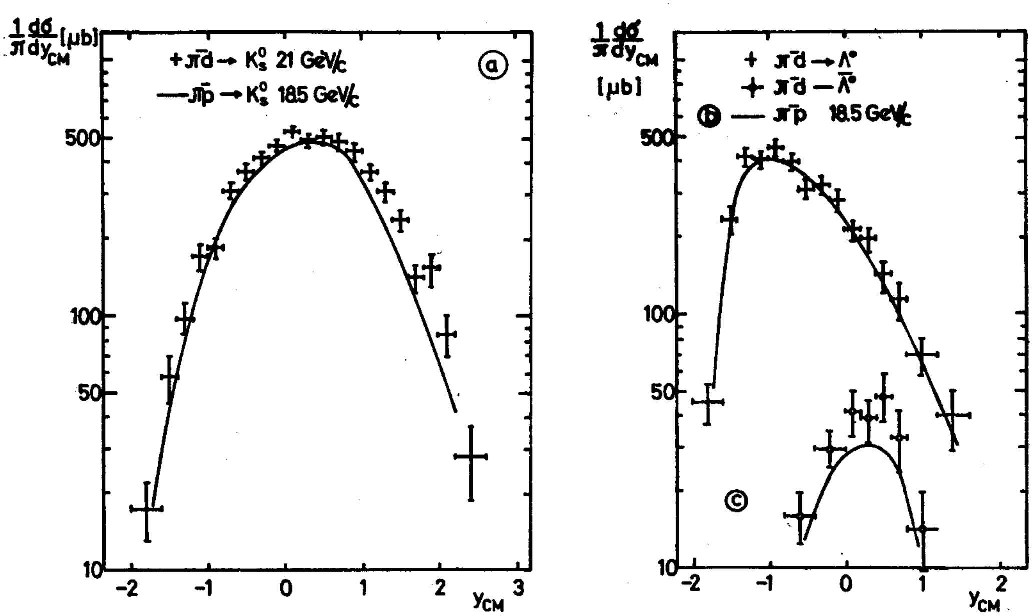

Fig. 3. Rapidity distributions for: a) K_S^0, b) Λ^0, c) $\bar{\Lambda}^0$. The solid lines are the data from π^-p 18.5 GeV/c [11]

value of A i.e. forward-backward asymmetry of K_S^0 and Λ^0 production decrease with increasing charge multiplicity both in π^-d and $\pi^{\pm}$p reactions as can be seen from Fig. 4.

These main properties of Λ^0, K_S^0 and $\bar{\Lambda}^0$ production in π^-d are also observed in the invariant distributions of the Feynman variable $x = \frac{P_L}{P_{max}}$

$$F(x) = \int \frac{E_{CM}}{\pi p_{max}} \frac{d^3\sigma}{dx dp_t^2} dp_t^2,$$

TABLE V

Asymmetry parameter A for neutral strange particle production in $\pi^{\pm}$p, $\pi^{\pm}$d and νp interactions

Reaction	A (K_S^0)	A (Λ^0)	A ($\bar{\Lambda}^0$)
π^-d 21 GeV	0.29 ± 0.02	-0.54 ± 0.02	0.27 ± 0.07
π^+d 24 GeV	0.28 ± 0.02	-0.51 ± 0.03	0.36 ± 0.10
π^-p 16 GeV	0.24 ± 0.02	-0.62 ± 0.02	0.22 ± 0.12
π^+p 16 GeV	0.32 ± 0.02	-0.56 ± 0.02	0.36 ± 0.09
νp 43 GeV	0.32 ± 0.02	-0.56 ± 0.02	

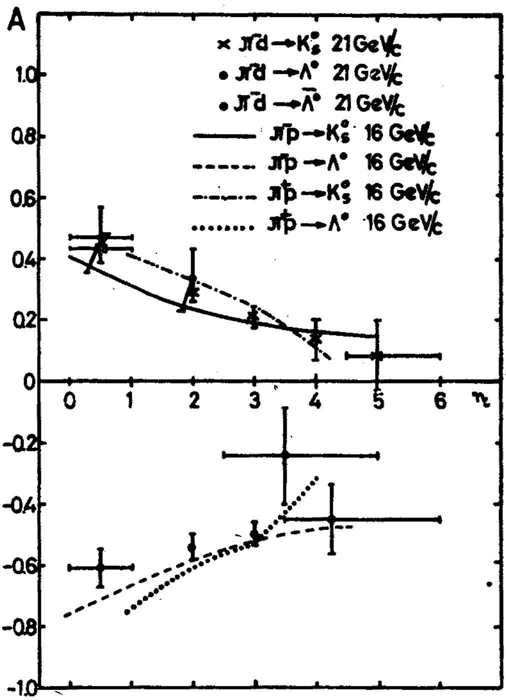

Fig. 4. Asymmetry parameter A as a function of the negative particle multiplicity associated with K_S^0, Λ^0, and $\bar{\Lambda}^0$ particle. The curves are the data from π^-p [10] and π^+p [19] interactions at 16 GeV/c

where P_L is the longitudinal CM momentum and P_{max} its maximum value for the reaction $\pi^- N \to \Lambda^0(K^0)$.

The invariant x distributions are shown in Fig. 5. The points for K_S^0 and Λ^0 produced in the backward hemisphere in π^-d reactions at 205 GeV [43] are included for comparison. The distributions for 21 and 205 GeV overlap within the large error bars, being consistent with an early scaling in K_S^0 and Λ^0 production in the target fragmentation region. The similarity of the longitudinal distributions for π^-p and π^-d suggests that nuclear effects in deuterium are not strong enough to be seen with the statistics available. The main characteristics of neutral strange particle production are also the same in $\pi^{\pm}p$ [1–23], π^+d [44] and pp [24–35] interactions. In contrast, the x distributions of K_S^0 and Λ^0 produced in K^-p interactions are essentially different as it can be seen from Fig. 5. The curves in Fig. 5 showing $F(x)$ for K^-p at 32 GeV [55] normalized to the same inclusive cross-section. The distribution of both K_S^0 and Λ^0 in K^-p interactions are shifted forward in CMS (much bigger $\langle x \rangle$). This can be explained by the presence of the valence s-quark (common to K^0 and Λ^0) in the K^- projectile. The distribution of $\bar{\Lambda}^0$ which does not contain the common

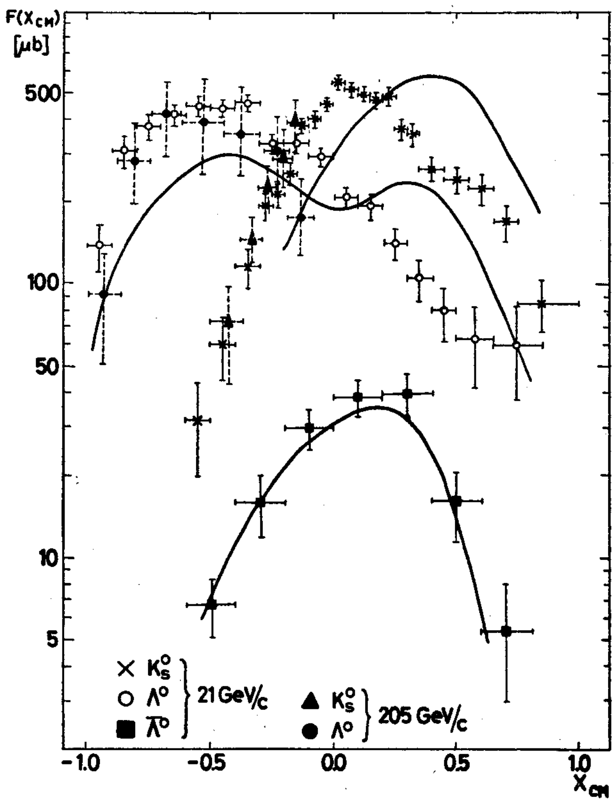

Fig. 5. Invariant $F(x)$ distributions for K_S^0, Λ^0 and $\bar{\Lambda}^0$ produced in π^-d interactions at 21 and 205 GeV/c [43]. The solid lines are the respective distributions for K^-p 32 GeV/c data [55] renormalized to the same inclusive cross-sections

valence quark with K^- remains the same in K^-p interactions as in collisions of non-strange hadrons.

The transverse momentum (P_t) distributions $\frac{d\sigma}{dp_t^2}$ of K_S^0, Λ^0, and $\bar{\Lambda}^0$ particles produced in π^-d interactions at 21 GeV are plotted in Fig. 6. The Λ^0 and $\bar{\Lambda}^0$ distributions can be well fitted by single exponent $A \cdot e^{-Bp_t^2}$ in the whole range available, i.e., up to 1.3 GeV^2/c^2 and 0.6 GeV^2/c^2, respectively. In contrast the K_S^0 distribution shows the characteristic change of slope at $p_t^2 \sim 0.5\ GeV^2/c^2$. At values of $p_t^2 > 0.5\ GeV^2/c^2$ the K_S^0 distribution closely follows the Λ^0 one, but for small p_t^2 values it can be parametrized by another simple exponential function with a bigger slope B. The fitted values of the parameters A and B together with the average p_t for Λ^0, K_S^0 and $\bar{\Lambda}^0$ are shown in Table VI.

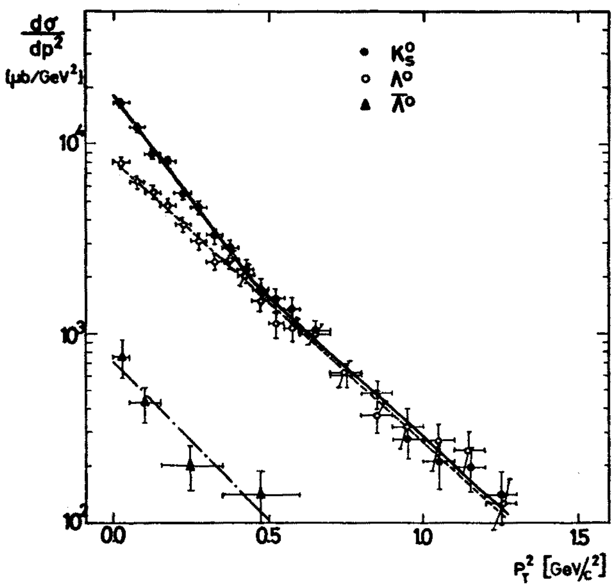

Fig. 6. Transverse momentum distributions for K_S^0 (full circles), Λ^0 (open circles) and $\bar{\Lambda}^0$ (triangles). The curves are fits $\frac{d\sigma}{dp_t^2} = A \cdot \exp(-Bp_t^2)$ with values of A and B given in Table VI. Solid line is for K_S^0, dashed line for Λ^0 and dashed-dotted line for $\bar{\Lambda}^0$

TABLE VI

The results of an exponential fit to $d\sigma/dp_t^2$ distributions of V^0 particles, together with average values of p_t

	K_S^0		Λ^0	$\bar{\Lambda}^0$
p_t^2 range [GeV/c^2]	0–0.5	0.5–1.4	0–1.4	0–0.6
A [mb/GeV^2]	18.11±0.55	9.68±2.11	8.46±0.29	0.70±0.15
B [GeV/c^{-2}]	5.05±0.16	3.55±0.28	3.50±0.09	4.0±0.8
χ^2/NDF	9.55/9	4.64/8	10.88/16	6.4/4
$\langle p_t \rangle$ [GeV/c]	0.417±0.006		0.478±0.009	0.46±0.02

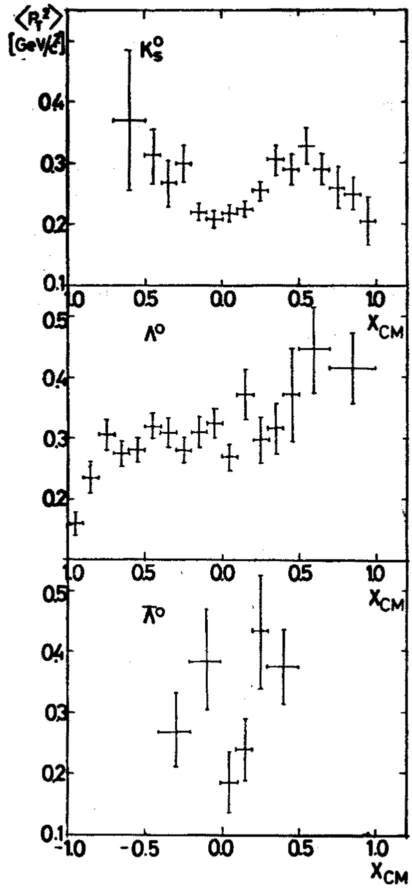

Fig. 7. Dependence of average transverse momentum squared $\langle p_t^2 \rangle$ on Feynman X for K_S^0, Λ^0, $\bar{\Lambda}^0$

Similar behaviour of $\frac{d\sigma}{dp_t^2}$ distribution for K_S^0 (and also for pions) has been observed in $\pi^{\pm}p$ and pp reactions at nearby energies [1–35]. It can be explained by resonance production, mainly K*(890). The K_S^0 particles coming from resonance decay have on the average a smaller p_t, causing an excess of K_S^0 inclusive cross-section at small p_t. The same break in slope is not observable for Λ^0 (which also partly come from the $\Sigma(1385)$ resonance decay) distribution, because of the smaller Q value of the $\Sigma(1385)$ resonance compared to K* and bigger mass of Λ^0 than K_S^0.

The values of slopes B as well as $\langle p_t \rangle$ obtained for π^-d reaction are for all neutral strange particles very similar to those observed in $\pi^{\pm}p$ and pp reactions in hydrogen experiments within a large energy range [1–35].

A correlation between the average p_t^2 and Feynman x variable is observed in Fig. 7 mainly for K_S^0 particles. This is the well known "sea-gull" effect [56], i.e. a dip in $\langle p_t \rangle$ at small $|x|$. It is significant for K_S^0, but hardly seen for Λ^0 and $\bar{\Lambda}^0$, as expected for more massive particles.

5. *Polarization of the lambda*

The polarization of Λ^0-hyperons has been calculated using the formula [57]

$$P = \frac{3}{\alpha}\langle\cos\theta\rangle,$$

where α is the asymmetry parameter of weak Λ^0 decay ($\alpha = 0.642$ [58]) and θ is the angle between the direction of the decay proton in the Λ^0 rest frame and the normal to the production plane $\hat{n}$

$$\hat{n} = \frac{\vec{P_\Lambda} \times \vec{P_{\pi^-}}}{|\vec{p_\Lambda} \times \vec{p_{\pi^-}}|},$$

$\vec{p_{\pi^-}}$, $\vec{p_\Lambda}$ are the momenta of the incident pion and Λ^0, respectively. The overall polarization of Λ^0 produced in the reaction $\pi^- d \to \Lambda^0 + \text{anything}$, $P_\Lambda = -0.06 \pm 0.06$, is consistent with zero. This is in agreement with the results from the $\pi^\pm p$ and pp experiments [1–35]. A more detailed analysis of polarization as a function of Λ^0 kinematic variables: Feynman x and p_t has been performed. It was found, that Λ^0 polarization is independent of x, fluctuating around zero for all values of x.

A double differential study of polarization turned out to be more interesting. For

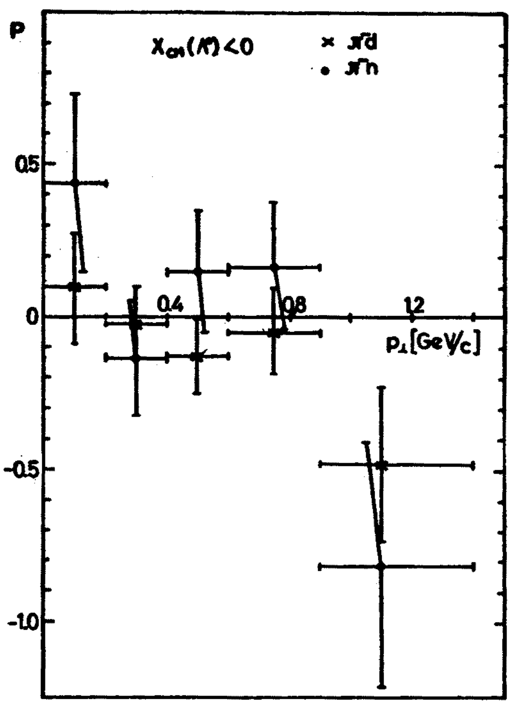

Fig. 8. Polarization of Λ^0 produced backward ($x < 0$) in π^-d (crosses) and π^-n (circles) interactions, as a function of Λ^0 transverse momentum p_t

$x < 0$, i.e. in the target fragmentation region, the Λ^0 polarization does depend on p_t as shown in Fig. 8. For $p_t \sim 1$ GeV/c the Λ^0 polarization becomes significantly negative both for the whole π^-d sample and the extracted π^-n interactions. This effect has been already observed in hydrogen experiments for the reactions πp, Kp, and pp [58] and quantitatively explained in different quark-parton models [59]. There is no significant p_t dependence of polarization for Λ^0 particles produced forward in CMS ($x > 0$) i.e. in π^- beam fragmentation region in π^-d data as well as in πp, pp experiments [58]. It seems that such an analysis allows one to extract the different Λ^0 production mechanisms which lead to negative Λ^0 polarization only in a specific kinematical regions. Our conclusions, however, are limited by insufficient statistics.

6. Associated production of neutral strange particles

In nonstrange hadronic collisions, such as π^-d each V^0 particle must be produced together with another strange particle due to strangeness conservation. The interesting question arises whether this conservation is local or only global. In this experiment only neutral strange particle pairs decaying inside the bubble chamber fiducial volume were available for the analysis. In Table II the inclusive cross-sections for $K^0_SK^0_S$, $K^0_S\Lambda^0$, $K^0_S\overline{\Lambda}^0$ and $\Lambda^0\overline{\Lambda}^0$ pairs are listed, as a function of associated charged multiplicity. Two dimensional scatter plots $\frac{d^2\sigma}{dy_1dy_2}$ are shown in Fig. 9a, b, c, d.

For $K^0_SK^0_S$ with the condition y_1 (on the horizontal axis) $> y_2$, the density of points in the plot is greatest for small $|y|$ of both kaons, which means the central production is dominant. However nearly in a half (45%) of observed pairs both K^0_S are forward in CMS and only in 13% of pairs both kaons are backward. This may indicate that the π^- fragmentation is also quite important in $K^0_SK^0_S$ pair production. This is also confirmed by the average values of rapidity: $\langle y_1 \rangle = 0.61 \pm 0.04$, $\langle y_2 \rangle = -0.11 \pm 0.04$. The average rapidity difference of the two kaons in each pair $\Delta y = y_1 - y_2$ which can be a measure of local strangeness conservation, amounts to $\langle \Delta y \rangle = 0.72 \pm 0.08$ indicating short range correlation in kaon pair production in π^-d interactions.

The events with detected $K^0_S\Lambda^0$ pair are particularly interesting since such K^0_S is known to be produced as K^0 (not $\overline{K}^0$ if one neglects the production of more than two strange particles at this rather low energy), whereas it is impossible to distinguish between K^0 and $\overline{K}^0$ in the inclusive K^0_S sample. It can be seen from Fig. 9b that in the overwhelming majority of the events (77%) Λ^0 is produced backward in CMS with the same average rapidity $\langle y_\Lambda \rangle = -0.54 \pm 0.04$ as for the full inclusive Λ^0 sample. The K^0 meson is produced mainly forward (68%) with the average rapidity $\langle y_K \rangle = 0.33 \pm 0.05$ also similar as for the full K^0_S sample. The most frequent configuration is forward K^0-backward Λ^0 (48%), but quite often (29%) both particles are produced backward, indicating that the contribution of target fragmentation process $N \to K^0\Lambda^0$ is important. The average distance in rapidity between K^0 and Λ^0 in a pair: $\Delta y = |y_K - y_\Lambda|$ is found to be $\langle \Delta y \rangle = 1.23 \pm 0.06$, much bigger than for $K^0_SK^0_S$ pairs. Thus, it seems, the strangeness conservation in the $K^0\Lambda^0$ pair production is not local and may imply some long range correlations.

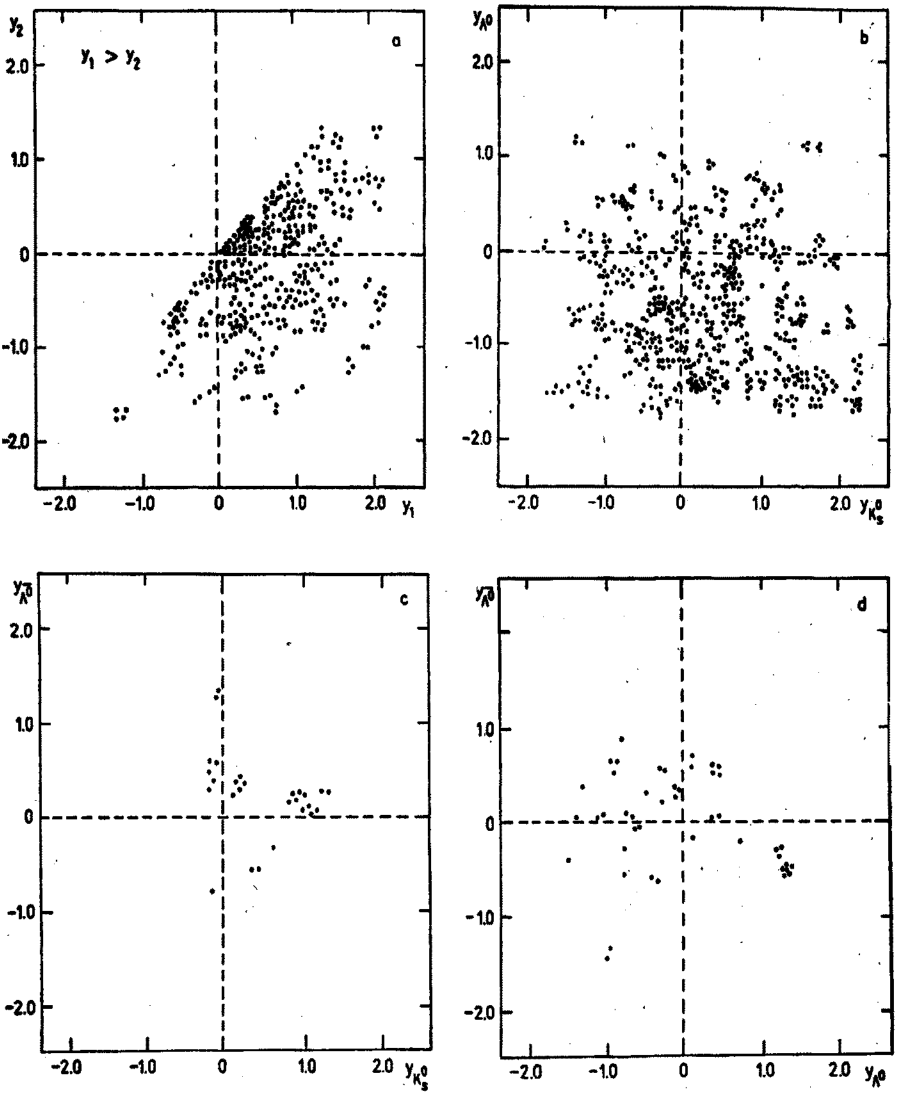

Fig. 9. Two-dimensional distributions of neutral strange particle pairs in terms of rapidity variable y: a) $K^0_SK^0_S$, b) $K^0_S\Lambda^0$, c) $K^0_S\bar{\Lambda}^0$, d) $\Lambda^0\bar{\Lambda}^0$

In $K^0_S\bar{\Lambda}^0$ pairs, there are only $\bar{K}^0$ produced. The majority of points on Fig. 9c lie in low rapidity region ($|y| < 1$). The central production of $\bar{K}^0\bar{\Lambda}^0$ pairs seems to be dominant, although the π^- beam fragmentation contribution must be significant since in most of the events (57%) both particles are produced forward and the average rapidities are: $\langle y_{\bar{K}} \rangle = 0.53 \pm 0.10$, $\langle y_{\bar{\Lambda}} \rangle = 0.31 \pm 0.11$. The mean value of $\Delta y = |y_{\bar{K}} - y_{\bar{\Lambda}}|$ is small: $\langle \Delta y \rangle = 0.62 \pm 0.08$. Thus similar short range correlations are observed as for the $K^0_SK^0_S$ pairs.

The $\Lambda^0\bar{\Lambda}^0$ pairs are produced centrally as can be seen from Fig. 9d. In most of the events (63%) Λ^0 and $\bar{\Lambda}^0$ go into the opposite CM hemispheres. A similar effect has been observed in $\pi^{\pm}$p interactions at 18.5 GeV [60] (64% of events for π^{+}p and 59% for π^{-}p) and π^{+}p at 16 GeV [19] (77%). The average rapidity of Λ^0 from $\Lambda^0\bar{\Lambda}^0$ pairs $\langle y_{\Lambda}\rangle = 0.02 \pm 0.14$ is totally different than that for the full inclusive Λ^0 sample ($\langle y_{\Lambda}\rangle = -0.51 \pm 0.02$). Thus the $\Lambda^0\bar{\Lambda}^0$ production mechanism must be essentially different than that for $K^0\Lambda^0$. The $\bar{\Lambda}^0$ particles are also produced much more centrally when in a pair with Λ^0 ($\langle y_{\bar{\Lambda}}\rangle = 0.04 \pm 0.11$) than in $\bar{\Lambda}^0\bar{K}^0$ pairs. The average rapidity distance $\Delta y = |y_{\Lambda} - y_{\bar{\Lambda}}|$ is smallest: $\langle \Delta y\rangle = 0.54 \pm 0.08$ which means more local strangeness compensation in $\Lambda^0\bar{\Lambda}^0$ production than for other neutral strange particle pairs.

The above analysis clearly shows the existence of short range rapidity correlation (local strangeness conservation) in neutral strange particle production in π^{-}d reaction at 21 GeV except on the $K^0\Lambda^0$ case. The range of this correlation decreases with increasing mass of the particles in a pair: $\langle \Delta y(K\bar{K})\rangle > \langle \Delta y(K\bar{\Lambda})\rangle > \langle \Delta y(\Lambda\bar{\Lambda})\rangle$. This seems to indicate that the correlation may, at least partly, come from the phase space constraints at such relatively low energy. However it should be noted that the local character of $K^0_S K^0_S$ production has been found in π^{-}p interactions at a much higher energy (205 GeV) [17].

7. The π^{-}n interactions and double scattering effects

An interaction of a negative pion with a neutron from deuterium target should lead to the odd number of produced charged particles in the final state, due to charge conservation. The proton remains a "spectator" and cannot be seen in the bubble chamber, if its Fermi momentum is small enough (less than 80 MeV/c). Thus in order to extract the events with neutral strange particles produced in π^{-}n interactions from the total π^{-}d sample, one can use the following experimental signature:

(*i*) odd charged particle multiplicity n_{ch},

(*ii*) even n_{ch}, but with visible proton spectator identified by ionization.

In the second class of events, we cannot rule out that the slow proton does not come from peripheral π^{-}p interactions or double scattering, unless it is emitted backward in LAB. However, even if in a V^0 event a sufficiently slow proton (below 500 MeV/c) does go forward, it is most probably a spectator, because the minimal momentum transfer necessary to produce a strange particle pair in π^{-}p reaction is too big to allow for such a slow recoil proton. Thus the experimental sample of π^{-}n interactions with V^0 production contains all single π^{-}n collisions with a small contamination of double scattering events.

The inclusive cross-sections for neutral strange particle production in π^{-}n interaction are shown in Table VII as a function of negative particle multiplicity. They have been calculated using only a clean sample of π^{-}n collisions, i.e. events with odd n_{ch} and events with even n_{ch}, but with proton spectator going backward in LAB, weighted by factor 2.15 resulting from the spectator angular distribution [47]. The inclusive cross-sections for K^0_S and Λ^0 are in agreement (within large error limit) with those found for isospin symmetric π^{+}p reaction at similar energies [11]. The $\bar{\Lambda}^0$ inclusive cross-section is bigger in π^{-}n 21 GeV than in π^{+}p 18.5 GeV. This difference may be understood in terms of the much stronger energy dependence of $\sigma(\bar{\Lambda}^0)$ than $\sigma(K^0_S)$ or $\sigma(\Lambda^0)$. From the interpolation

TABLE VII

Semi-inclusive cross-sections for neutral strange particle production in π^-n interactions vs negative particle multiplicity n_-

n_-	1	2	3	4	5	6	Total
$\sigma_{incl}(K_S^0)$ [μb]	303±26	485±37	386±30	112±13	22±5	3±1	1293±85
$\sigma_{incl}(\Lambda^0)$ [μb]	145±15	296±25	245±22	98±12	27±6	2±1	813±58
$\sigma_{incl}(\overline{\Lambda}^0)$ [μb]	20±7	30±5	13±3	6±2			69±9

of the data in Fig. 2c one could expect a 15% increase of $\sigma(\overline{\Lambda}^0)$ from 18 to 21 GeV. Bigger difference is probably caused by symmetric errors in both experiments.

In order to estimate the amount of double scattering in neutral strange particle production the parameter f, usually defined for total inelastic cross-sections [47], has been calculated

$$f = \frac{\sigma_{\pi^-d}(V^0) - \sigma^d_{\pi^-n}(V^0) - \sigma^d_{\pi^-p}(V^0)}{\sigma_{\pi^-d}(V^0)},$$

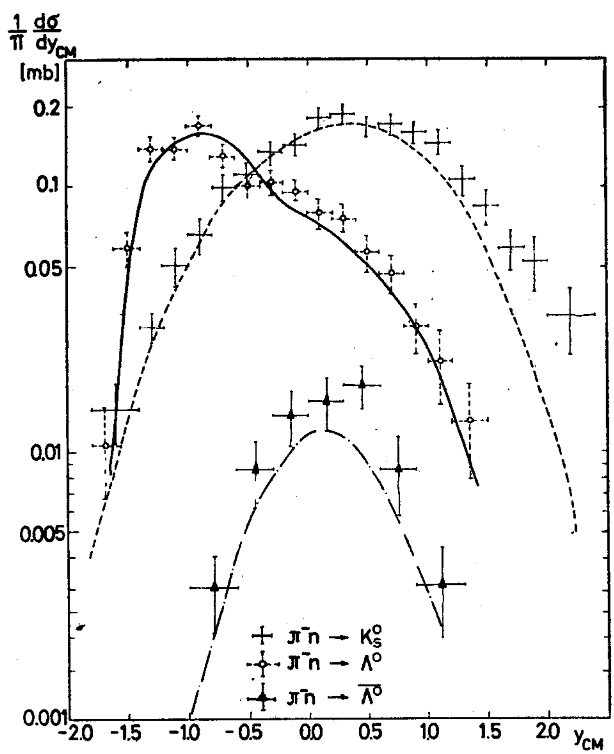

Fig. 10. Rapidity distributions of V° particles produced in π^-n interactions, compared with π^+p 18.5 GeV/c [11] data (solid line for Λ^0, dashed line for K_S^0 and dashed-dotted line for $\overline{\Lambda}^0$)

where $\sigma_{\pi^-d}(V^0)$, $\sigma^d_{\pi^-n}(V^0)$, $\sigma^d_{\pi^-p}(V^0)$ are the inclusive cross sections for V^0 production in π^-d interactions, single collisions with neutron from deuterium target, and single collisions with proton from deuteron, respectively. The values of $\sigma_{\pi^-d}(V^0)$ and $\sigma^d_{\pi^-n}(V^0)$ have been determined in this experiment (Tables I and VII, respectively). The cross-section for V^0 production in single collisions with proton $\sigma^d_{\pi^-p}(V^0)$ can be estimated from the interpolation of hydrogen π^-p data. The contribution of the double scattering to the inclusive neutral strange particle cross-sections obtained in this way are following: $f(K^0_S) = 16 \pm 7\%$, $f(\Lambda^0) = 21 \pm 8\%$. For $\bar{\Lambda}^0$ the statistics is too small to get any significant result. It seems that nuclear effects are of the similar order in the inclusive production of K^0_S and Λ^0 as for the total inelastic π^-d cross-sections at 21 GeV/c ($f = 16 \pm 1\%$ found in Ref. [61]).

The inclusive V^0 distributions have been obtained for the "π^-n" sample selected in the described way, i.e. containing events of single π^-n scattering with negligible contamination of double scattering. In order to get full V^0 sample produced in π^-n interactions one has to correct for all those double scattering events in which V^0's were produced in the first collision with the neutron. This could not be done experimentally, however one can expect that this correction is less than 10% from the estimated total amount of double scattering.

The rapidity distributions of K^0_S, Λ^0 and $\bar{\Lambda}^0$ produced in π^-n interactions are shown in Fig. 10 together with the curves for the hydrogen π^+p data at 18.5 GeV [11]. The distribu-

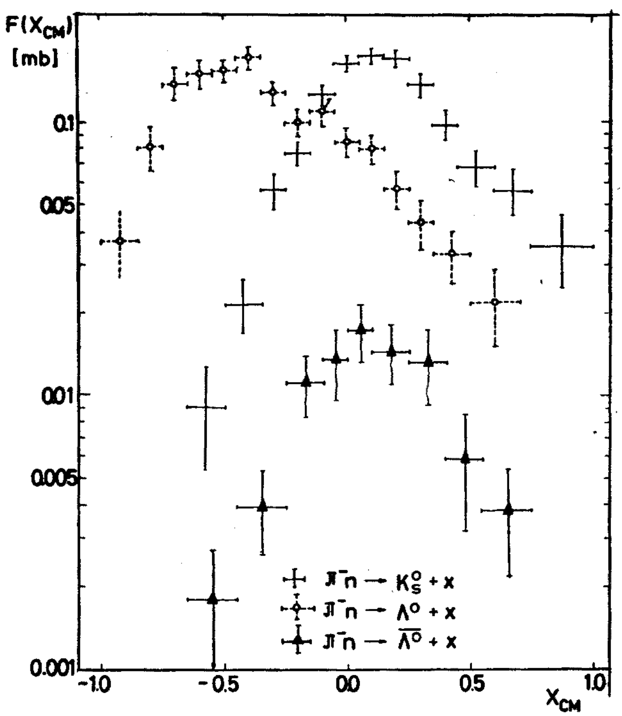

Fig. 11. Invariant $F(x)$ distributions for K^0_S (crosses), Λ^0 (circles) and $\bar{\Lambda}^0$ (triangles) produced in π^-n interactions

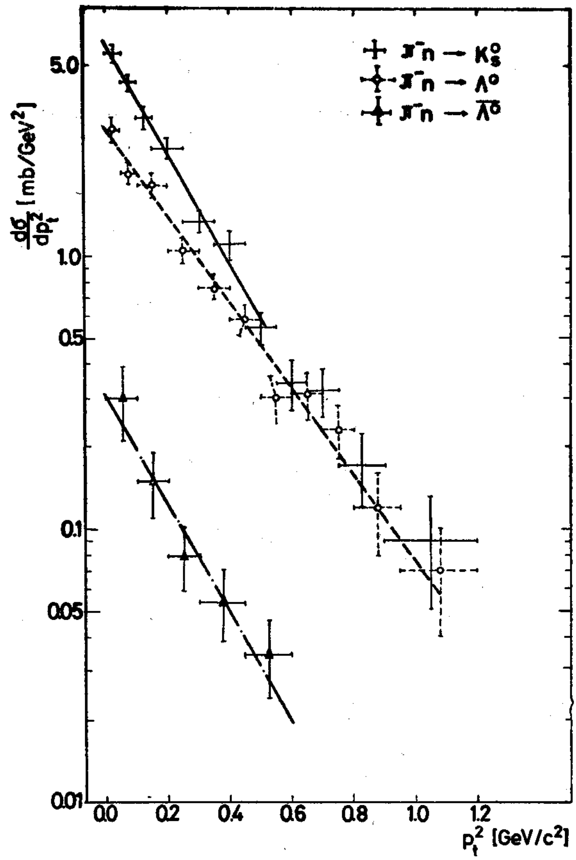

Fig. 12. Transverse momentum distributions for K_S^0 (crosses), Λ^0 (circles) and $\bar{\Lambda}^0$ (triangles) produced in π^-n interactions. The curves are $A \cdot \exp(-Bp_t^2)$ fits with A and B values given in Table VIII

tion is very similar for π^-n and the isospin-symmetric π^+p reaction; also the shapes of $\bar{\Lambda}^0$ distributions are the same for both reactions only the normalization being different due to the bigger $\bar{\Lambda}^0$ inclusive cross-section in π^-n than in π^+p reaction. The distribution for K_S^0 is the same for π^-n as for π^+p in the target fragmentation and central regions, but different for fast particles with rapidities greater than 1. The points for π^-n are significantly above π^+p in the beam fragmentation region. This difference can be explained in the framework of the quark-parton model. The observed K_S^0 state originates from K^0 or $\bar{K}^0$ produced in a strong interaction conserving strangeness quantum number. K^0 is produced more often since it can be associated with hyperon, whereas $\bar{K}^0$ predominantly with K^0. K^0 particle having one common valence quark $\bar{u}$ with π^- beam and no common quark with π^+ is produced more forward and with a higher average y in π^- induced reaction than in the case of the π^+ beam.

The invariant $F(x)$ distributions of K_S^0, Λ^0 and $\bar{\Lambda}^0$ produced in π^-n reaction, shown in Fig. 11 look very similar as for the whole π^-d sample (Fig. 5) with K_S^0 and $\bar{\Lambda}^0$ produced mainly in the central and beam fragmentation regions, while Λ^0 comes mostly from the

TABLE VIII

The results of an exponential fit to $\frac{d\sigma}{dp_t^2}$ distributions of V^0 particles produced in π^-n interactions

	K_S^0	Λ^0	$\bar{\Lambda}^0$
p_t^2 range [GeV/c^2]	0–0.5	0–1.2	0–0.6
χ^2/NDF	6.96/6	9.27/9	2.7/5
A [mb/GeV^2]	6.13 ± 0.31	2.92 ± 0.18	0.31 ± 0.09
B [GeV/c^{-2}]	4.73 ± 0.23	3.69 ± 0.19	4.69 ± 1.0

neutron fragmentation. Also the $d\sigma/dp_t^2$ distributions for all neutral strange particles produced on neutrons (Fig. 12) have the same exponential shape as for the π^-d reaction, K_S^0 having the characteristic change of slope at 0.5 GeV^2/c^2. The results of the exponential fit $A \cdot \exp(-Bp_t^2)$ (curves on Fig. 12) are summarized in Table VIII. The slopes B for K_S^0 and Λ^0 are similar for the π^-n, $\pi^\pm p$ and π^-d reactions. In the $\bar{\Lambda}^0$ case the statistical errors are large but $d\sigma/dp_t^2$ distribution in π^-n seems to decrease faster than for K_S^0 and Λ^0.

8. *Fragmentation processes — comparison with quark counting rules*

In the low-p_t π^-d interactions measured in this experiment, it was possible to analyse several one-particle fragmentation processes both in the beam and target C.M. hemispheres:

a) $\pi^- \to K_S^0$,

b) $\pi^- \to \Lambda^0$,

c) $\pi^- \to \bar{\Lambda}^0$,

d) $d \to K_S^0$,

e) $d \to \Lambda^0$,

f) $d \to \bar{\Lambda}^0$.

Using the procedure described in Chapter VII the neutron fragmentation into neutral strange particles could be extracted from deuterium data:

g) $n \to K_S^0$,

h) $n \to \Lambda^0$,

i) $n \to \bar{\Lambda}^0$.

Also fragmentation into proton has been analyzed in the region $x < -0.7$ for the sake of comparison:

j) $n \to p$.

The data for the reaction j) have been obtained by measuring slow protons (identified by ionization) produced in $\pi^- n$ collisions, i.e. in events with odd multiplicity and slow proton or even multiplicity and two slow protons (the slower one was assumed to be spectator).

The invariant $F(x)$ distributions (integrated over p_t) for all target fragmentation processes (d–j) are shown in Fig. 13a and for beam fragmentation processes (a–c) in Fig. 13b. All $F(x)$ distributions are adequately fitted by $(1-|x|)^n$ function (curves in Fig. 13) as predicted by most of the quark models of low p_t hadronic interactions (see for the review [62]). The fitted values of the power n together with the range of x, χ^2/NDF of the fit and the Quark Counting Rule predictions [63] are summarized in Table IX.

Quark Counting Rules (QCR) are simple rules determining the power n in the $(1-|x|)^n$ dependence of $F(x)$ distributions experimentally observed in many hadron fragmentation processes $h \to h'$ at $|x| \to 1$ [62, 64]. The value of n is given according to these rules, by the quark content of the observed particle h′ and of the fragmenting hadron h. In this paper QCR formulated by Gunion [63] are used for comparison with the data. Thus the predicted value of n is given by the formula:

$$n = 2n_H + n_{PL} - 1,$$

where n_H is the number of "passive" spectator quarks present already in a minimal initial hadron state and n_{PL} counts quarks taking part in the point-like creation of additional,

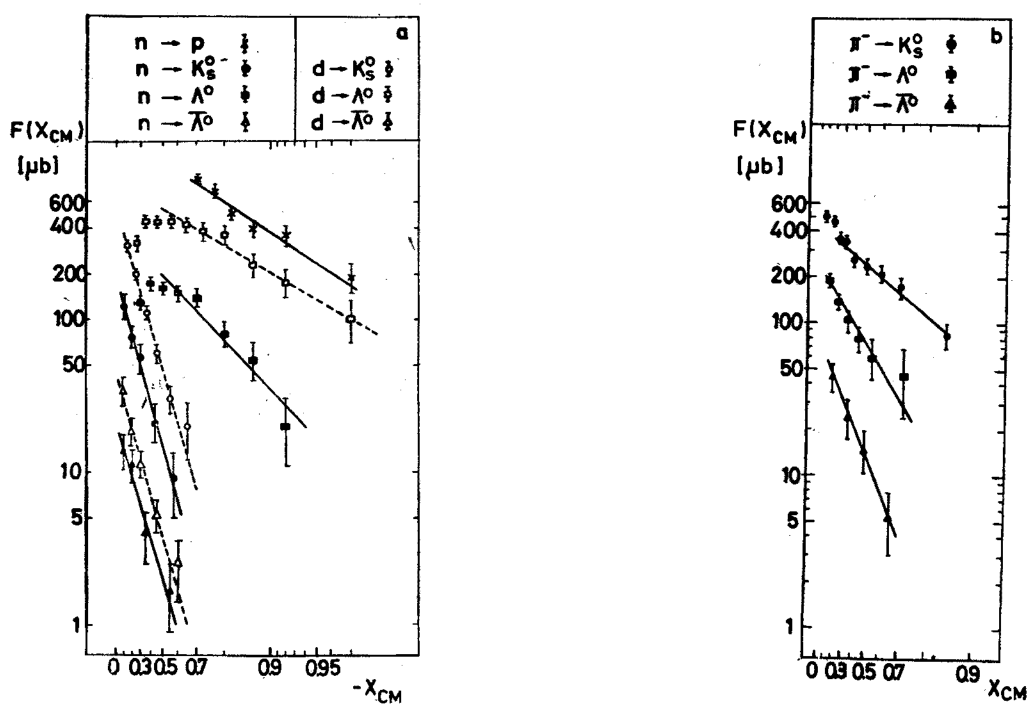

Fig. 13. Invariant $F(x)$ distributions for: a) target fragmentation processes, b) beam fragmentation processes. The curves are fits to $(1-|x|)^n$ dependence

TABLE IX

The results of $(1-|x|)^n$ fit to $F(x)$ distributions for various fragmentation processes together with Quark Counting Rules predictions (n_{th})

Process	Range of x	χ^2/NDF	n_{exp}	n_{th} QCR
$\pi^- \to K_S^0$	0.25 — 1.0	4.3/6	0.88 ± 0.12	1
$\pi^- \to \Lambda^0$	0.1 — 0.9	4.0/5	1.71 ± 0.37	2
$\pi^- \to \bar{\Lambda}^0$	0.1 — 0.8	2.1/4	2.50 ± 0.48	2
$d \to K_S^0$	−0.7 — −0.1	3.5/5	3.62 ± 0.27	3.5
$d \to \Lambda^0$	−1.0 — −0.6	2.2/6	0.59 ± 0.12	1
$d \to \bar{\Lambda}^0$	−0.7 — −0.1	2.3/4	3.97 ± 1.09	5
$n \to K_S^0$	−0.7 — −0.1	2.2/5	3.67 ± 0.36	3
$n \to \Lambda^0$	−1.0 — −0.5	5.2/6	1.02 ± 0.15	1
$n \to \bar{\Lambda}^0$	−0.7 — −0.1	3.2/4	3.42 ± 0.89	5
$n \to p$	−1.0 — −0.7	4.0/6	0.68 ± 0.15	1

necessary partons to form a hadron h'. The QCR prediction for reactions $\pi^- \to K_S^0$ and $n \to K_S^0$ is given in Table IX, the same as for fragmentation into K^0, assuming negligible $\bar{K}^0$ production in both π^- and n fragmentation regions ($\bar{K}^0$ has no common valence quarks with π^- and neutron). The QCR predicts $n = 3$ for $n \to K^0$ and $n = 4$ for $p \to K^0$, thus for deuteron fragmentation $d \to K_S^0$ the average value $n = 3.5$ is predicted, assuming no nuclear effects and neglecting again the $\bar{K}^0$ production.

One can conclude from Table IX that there is quite satisfactory general agreement between data and model predictions, although the statistical errors are big and model assumptions (neglecting $\bar{K}^0$ production and nuclear effects) are crude. The influence of resonance production on the observed particle spectra is also unclear and may be significant especially at small $|x|$. The limited statistics for large $|x|$ and the difficulties with clear distinction between central and fragmentation regions at this rather low energy make the comparison with QCR even more difficult. For some of the reactions the fragmentation region has been defined as $|x| > 0.1$. Thus the model assumption $|x| \to 1$ is probably not satisfied well enough.

The obtained value of n, for $d \to \Lambda^0$ fragmentation significantly lower than predicted (and similarly for $n \to p$), is consistent with the results found in other deuterium and hydrogen experiments [64]. This confirm the indication that the QCR seem to work less exactly in case of baryon-baryon fragmentation. The observed value of the power n for $\bar{\Lambda}^0$ is also smaller than QCR prediction, but the errors are too large to draw any stronger conclusions.

9. *Summary and conclusions*

The inclusive cross-sections for neutral strange particle production in π^-d interactions at 21 GeV/c are: $\sigma(K_S^0) = 3671 \pm 195$ μb, $\sigma(\Lambda^0) = 2381 \pm 131$ μb, $\sigma(\bar{\Lambda}^0) = 192 \pm 18$ μb. The topological cross-sections have also been found. The determined average production rate of V^0 particles per inelastic collision: $\langle K_S^0 \rangle = 0.096 \pm 0.006$, $\langle \Lambda^0 \rangle = 0.062 \pm 0.004$, $\langle \bar{\Lambda}^0 \rangle = 0.0048 \pm 0.0006$ are in agreement with those found in hydrogen $\pi^- p$ experiments at similar energies. The excess of strange particle production in deuterium is seen only in higher multiplicity events for which nuclear effects are known to be stronger.

The main dynamical features of neutral strange particle production in $\pi^- d$ interactions at 21 GeV are the same as in elementary collisions of nonstrange hadrons ($\pi^\pm p$ and pp) at similar energies, i.e. K_S^0 and $\bar{\Lambda}^0$ are produced mainly in the central and beam fragmentation regions, whereas Λ^0 hyperon comes mostly from the nucleon (target) fragmentation process with some contribution of central production. Also the p_t^2 dependence of V^0 production seems to be universal for the interactions all hadrons with proton and deuteron.

The strangeness conservation is local in rapidity in the $K^0\bar{K}^0$, $\bar{K}^0\bar{\Lambda}^0$ and $\Lambda^0\bar{\Lambda}^0$ pair production, whereas $K^0\Lambda^0$ production exhibits some long range rapidity correlation.

The Λ^0 polarization is negligible for the whole $\pi^- d$ sample. Significant negative polarization of Λ^0 particles produced in the target fragmentation region with $p_t \sim 1$ GeV/c is, however, observed in qualitative agreement with quark-parton model predictions.

The inclusive cross-sections and one-particle distributions of K_S^0, Λ^0 and $\bar{\Lambda}^0$ produced in $\pi^- n$ reaction are found to be similar to those in the isospin-symmetric $\pi^+ p$ reaction except for the $\pi^- \to K_S^0$ fragmentation which has different y dependence than $\pi^+ \to K_S^0$ as expected in the quark-parton model.

The double scattering contribution to the K_S^0 ($16 \pm 7\%$) and Λ^0($21 \pm 8\%$) production is estimated. This is in agreement with the value ($16 \pm 1\%$) found previously for the total inelastic $\pi^- d$ cross-sections.

The invariant $F(x)$ distributions of V^0 particles in both beam and target fragmentation regions are well fitted by the $(1-|x|)^n$ dependence. The experimental values of the power n are in good agreement with the Gunion quark counting rule predictions, except in the process $d \to \Lambda^0$ and $n \to p$ for which n is lower (~ 0.6) than predicted (1.0). It seems that nuclear effects in deuterium do not significantly influence the $F(x)$ distributions in fragmentation regions.

The author gratefully acknowledges the work of CERN PS-beam staff, scanning and measuring teams in Cambridge, Cracow and Warsaw laboratories.

The author thanks all Colleagues from Cracow Bubble Chamber Group for helpful discussions, in particular prof. A. Eskreys for continuous support and dr T. Coghen for many useful comments.

REFERENCES

[1] O. Goussu et al., *Nuovo Cimento* **42A**, 606 (1966).
[2] T. Wangler et al., *Phys. Rev.* **B137**, 414 (1965).
[3] J. Bartsch et al., *Nuovo Cimento* **43A**, 1010 (1966).
[4] L. Bertanza et al., *Phys. Rev.* **130**, 786 (1963).
[5] V. Glagolev et al., JINR P1-8147 74 Dubna.
[6] M. Soloviev et al., Proc. Rochester Conf. 1960, p. 388.
[7] A. Bigi et al., *Nuovo Cimento* **33**, 1246 (1964).
[8] T. Ferbel, H. Taft, *Nuovo Cimento* **28**, 1214 (1963).

[9] F. Barreiro et al., *Phys. Rev.* **D17**, 669 (1978).
[10] E. Balea et al., *Nucl. Phys.* **B163**, 21 (1980).
[11] P. Stuntebeck et al., *Phys. Rev.* **D9**, 608 (1974).
[12] E. Balea et al., *Rev. Roum. Phys.* **15**, 587 (1970).
[13] N. Angelov et al., *Yad. Fiz.* **34**, 1234 (1981).
[14] N. Biswas et al., *Nucl. Phys.* **B167**, 41 (1980).
[15] D. Brick et al., *Phys. Rev.* **D20**, 2124 (1979).
[16] D. Ljung et al., *Phys. Rev.* **D15**, 3163 (1977).
[17] D. Bogart et al., *Phys. Rev.* **D16**, 2008 (1977).
[18] R. Tost et al., *Nucl. Phys.* **B63**, 248 (1973).
[19] P. Bosetti et al., *Nucl. Phys.* **B94**, 21 (1975).
[20] A. Ajinenko et al., *Nucl. Phys.* **B165**, 1 (1980).
[21] R. Alston et al., *Phys. Rev. Lett.* **35**, 142 (1975).
[22] D. Brick et al., *Nucl. Phys.* **B164**, 1 (1980).
[23] K. Böckmann et al., *Nucl. Phys.* **B166**, 284 (1980).
[24] R. Eisner et al., *Nucl. Phys.* **B123**, 361 (1977).
[25] K. Maeger et al., *Phys. Rev.* **D11**, 1756 (1975).
[26] K. Alpgard et al., *Nucl. Phys.* **B105**, 349 (1976).
[27] H. Boggild et al., *Nucl. Phys.* **B57**, 77 (1973).
[28] E. Blumen et al., *Nucl. Phys.* **B125**, 253 (1977).
[29] G. Blobel et al., *Phys. Lett.* **48B**, 73 (1974).
[30] D. Chapmann et al., *Phys. Lett.* **47B**, 465 (1973).
[31] S. Sheng et al., *Phys. Rev.* **D11**, 1733 (1975).
[32] F. Dao et al., *Phys. Rev. Lett.* **30**, 1151 (1973).
[33] J. Bartke et al., *Nuovo Cimento* **29**, 8 (1963).
[34] N. Ammosov et al., *Nucl. Phys.* **B115**, 269 (1976).
[35] R. Charlton et al., *Phys. Rev. Lett.* **30**, 574 (1973).
[36] E. Handler et al., *Nucl. Phys.* **B110**, 173 (1976).
[37] P. Carlson et al., *Nucl. Phys.* **B99**, 451 (1975).
[38] F. Dao et al., *Phys. Lett.* **51B**, 505 (1974).
[39] M. Jabiol et al., *Nucl. Phys.* **B127**, 365 (1977).
[40] D. Ward et al., *Phys. Lett.* **62B**, 237 (1976).
[41] D. Drijard et al., *Z. Phys.* **C12**, 217 (1982).
[42] K. Alpgard et al., *Phys. Lett.* **115B**, 65 (1982).
[43] S. Csorna et al., *Nucl. Phys.* **B124**, 19 (1977).
[44] S. Dado et al., *Phys. Rev.* **D22**, 2656 (1980).
[45] V. Bakken et al., *Nuovo Cimento* **A66**, 71 (1981).
[46] C. Hochman et al., *Nucl. Phys.* **B89**, 383 (1975).
[47] R. Ansorge et al., *Nucl. Phys.* **B109**, 197 (1976).
[48] F. Bruyant et al., CERN Computer 6000 Series Program Library Long Write Up X-201 (1968).
[49] E. Beck et al., CERN Computer 6000 Series Program Library Long Write Up X-601 (1968).
[50] J. Podolański, R. Armenteros, *Philos. Mag.* Series 7, **45**, 13 (1954).
[51] A. Wróblewski *Acta Phys. Pol.* **B4**, 857 (1973).
[52] E. Kladnitskaya, *Fiz. Elem. Chastits & At. Yadra* **13**, 669 (1982).
[53] L. Hulthén, M. Sugawara, *Handbuch der Physik*, Vol. 39, Springer-Verlag, Berlin 1957, p. 1.
[54] H. Graessler et al., *Nucl. Phys.* **B194**, 1 (1982).
[55] U. Gensch et al., *Nucl. Phys.* **B173**, 154 (1980).
[56] M. Bardadin-Otwinowska et al., *Phys. Lett.* **21**, 351 (1966).
[57] W. T. Eadie et al., *Statistical Methods in Experimental Physics*, North Holland Pub. Comp., Amsterdam–London 1971, p. 153.
[58] G. Bunce et al., *Phys. Rev. Lett.* **36**, 1113 (1976); S. Erhan et al., *Phys. Lett.* **82B**, 301 (1979).

[59] J. Szwed, *Phys. Lett.* **B105**, 403 (1981); De Grand, H. Miettinen, HU-TFT-81-35; B. Andersson, G. Gustafson, G. Ingleman, *Phys. Lett.* **B85**, 417 (1979).
[60] P. Lichtmayet et al., *Nucl. Phys.* **B105**, 229 (1976).
[61] A. Eskreys et al., *Nucl. Phys.* **B173**, 93 (1980).
[62] K. Fiałkowski, W. Kittel, *Rep. Prog. Phys.* **46**, 1283 (1983).
[63] J. Gunion, *Phys. Lett.* **88B**, 150 (1979).
[64] D. Denegri et al., *Phys. Lett.* **98B**, 127 (1981).